Original Article

Association of epicardial fat volume with subclinical myocardial damage in patients with type 2 diabetes mellitus

Yurui Hu[1,2#], Wenji Yu[1,2#], Feifei Zhang[1,2], Yufeng Wang[1,2], Jingwen Wang[1,2], Peng Wan[3], Xiaoliang Shao[1,2], Jianfeng Wang[1,2], Yonghong Sun[1,2], Yuetao Wang[1,2]^

[1]Department of Nuclear Medicine, The Third Affiliated Hospital of Soochow University, Changzhou, China; [2]Institute of Clinical Translation of Nuclear Medicine and Molecular Imaging, Soochow University, Changzhou, China; [3]Department of Cardiology, The Third Affiliated Hospital of Soochow University, Changzhou, China

Contributions: (I) Conception and design: Y Hu, W Yu, Yuetao Wang; (II) Administrative support: Yuetao Wang; (III) Provision of study materials or patients: F Zhang, Jingwen Wang; (IV) Collection and assembly of data: Y Hu, Yufeng Wang; (V) Data analysis and interpretation: P Wan, X Shao, Jianfeng Wang, Y Sun; (VI) Manuscript writing: All authors; (VII) Final approval of manuscript: All authors.

[#]These authors contributed equally to this work as co-first authors.

Correspondence to: Yuetao Wang, MD. Department of Nuclear Medicine, The Third Affiliated Hospital of Soochow University, 185, Juqian Street, Changzhou 213003, China; Institute of Clinical Translation of Nuclear Medicine and Molecular Imaging, Soochow University, Changzhou, China. Email: yuetao-w@163.com.

Background: In type 2 diabetes mellitus (T2DM) patients, left ventricular systolic dyssynchrony (LVSD) with normal left ventricular ejection fraction (LVEF) and normal myocardial perfusion could referred to as subclinical myocardial damage, which is difficult to diagnose at an early stage. Epicardial adipose tissue, a distinctive heart-specific visceral fat, is closely related to various cardiovascular diseases. The objective of this study was to investigate the correlation between epicardial fat volume (EFV) and subclinical myocardial damage in T2DM patients.

Methods: This retrospective cross-sectional study included 117 T2DM patients with normal myocardial perfusion by single photon emission computed tomography-computed tomography (SPECT-CT) and normal LVEF by echocardiography. The study was conducted from January 2018 to December 2022. Patient data were collected through electronic medical records including basic patient information, medical history, laboratory tests, and medication data. The EFV was quantified through a non-contrast CT scan. Quantitative indicators of LVSD including phase standard deviation (PSD) and phase histogram bandwidth (PBW) were obtained through phase analysis of the gated rest myocardial perfusion imaging (MPI). Additionally, 83 healthy individuals at the same time were selected to gain the reference threshold of LVSD indicators (13.1° for PSD and 37.6° for PBW). Univariate and multivariable logistic regression models were performed to analyze factors influencing LVSD. A generalized additive model (GAM) was applied to explore the relationship between EFV and LVSD. The receiver operating characteristic (ROC) curve was used to analyze the diagnostic value of EFV for LVSD.

Results: Among all patients, 32 (27.4%) patients had LVSD. Compared with the non-LVSD group, the body mass index (BMI) and EFV were higher in the LVSD group (25.83±2.66 *vs.* 23.94±3.13 kg/m^2; 142.41±44.17 *vs.* 108.01±38.24 cm^3, respectively, both P<0.05). Multivariate regression analysis revealed that EFV was independently associated with LVSD [odds ratio (OR) =1.19; 95% confidence interval (CI): 1.06–1.34; P=0.003]. Age, BMI, incidence of hypertension, and LVSD were increased with tertiles of EFV

^ ORCID: 0000-0003-2859-8625.

(all P<0.05). The GAM indicated a linear association between EFV and LVSD. The ROC curve analysis concluded that the area under the curve (AUC) of EFV for predicting subclinical myocardial damage in T2DM patients was 0.732 (95% CI: 0.633–0.831, P<0.001), with the optimal threshold of 122.26 cm^3, sensitivity of 71.9%, and specificity of 69.4%.

Conclusions: EFV is an independent risk factor for LVSD in T2DM patients with normal LVEF and normal MPI, which could potentially serve as a novel imaging marker and a potential therapeutic target for subclinical myocardial damage.

Keywords: Epicardial fat volume (EFV); type 2 diabetes mellitus (T2DM); gated myocardial perfusion imaging (GMPI); left ventricular systolic dyssynchrony (LVSD); subclinical myocardial damage

Submitted Oct 10, 2023. Accepted for publication Jan 22, 2024. Published online Mar 07, 2024.
doi: 10.21037/qims-23-1413
View this article at: https://dx.doi.org/10.21037/qims-23-1413

Introduction

Based on the data provided by the International Diabetes Federation (IDF), the worldwide occurrence of type 2 diabetes mellitus (T2DM) in individuals aged 20 to 79 years was estimated to be 10.5% (536.6 million individuals) in the year 2021 (1). Diabetic cardiomyopathy, a major diabetic cardiovascular complication, is the leading cause of morbidity in T2DM, characterized by systolic function impairment and difficulties in early diagnosis (2). Left ventricular ejection fraction (LVEF) is the most common clinical parameter for quantifying global ventricular systolic function. However, due to the compensatory mechanism, at the initial stages of diabetic cardiomyopathy, the LVEF could be preserved (3). A study showed that in the early stage, diabetic cardiomyopathy patients had normal myocardial perfusion, with alterations in mitochondrial, myocardial, and metabolic, and function, whereas the abnormality of myocardial perfusion and LVEF eventually appeared in the late stage (4). Our previous study found that left ventricular systolic dyssynchrony (LVSD) was present among 21.1% of individuals with T2DM who exhibited normal LVEF and normal myocardial perfusion, which is also known as subclinical myocardial damage, and need early intervention to improve poor prognosis. Besides, we also found that overweight is closely correlated with subclinical myocardial damage (5).

LVSD refers to losing synchronicity of mechanical contraction in different segments of the left ventricle (6). Several imaging techniques can be used to assess left ventricle synchronization, including single photon emission computed tomography-computed tomography (SPECT-CT), cardiac magnetic resonance imaging (MRI), and echocardiography. MRI is expensive and involves intricate operations. In addition, some patients with metal implants are contraindicated for MRI. Echocardiography is operator dependent and may have low accuracy in patients with a poor acoustic window. SPECT-CT is a widely used, cost-effective, non-invasive imaging modality that facilitates simultaneous evaluation of myocardial perfusion and left ventricular systolic synchrony with good repeatability. LVSD significantly contributes to both the pathologic process of heart failure (HF) and ventricular remodeling (7,8).

Epicardial adipose tissue (EAT) is the visceral fat depot of the heart, mainly surrounding major epicardial coronary arteries or the myocardium, which can be quantitatively assessed according to epicardial fat volume (EFV) by SPECT-CT and has been considered as a promising risk indicator for cardiovascular disease (9). Studies have shown a significant association between EFV and various cardiovascular conditions, including atherosclerosis, coronary artery disease, HF, and atrial fibrillation (10-12). A study on adults with uncomplicated obesity found that visceral adipose tissue was independently associated with left ventricular global longitudinal systolic strain (GLS), a marker of early subclinical left ventricular dysfunction (13). Besides, a transformation in lifestyle habits or medicinal interventions (statins or dapaglifozin) can proficiently mitigate the accumulation of EFV (14), which highlights the potentiality of EAT as a therapeutic target. However, the relationship between EAT and subclinical myocardial impairment among T2DM patients remains uncertain.

Thus, the aim of this study was to explore the correlation between EFV and LVSD in T2DM patients with normal LVEF and normal myocardial perfusion, which may be a

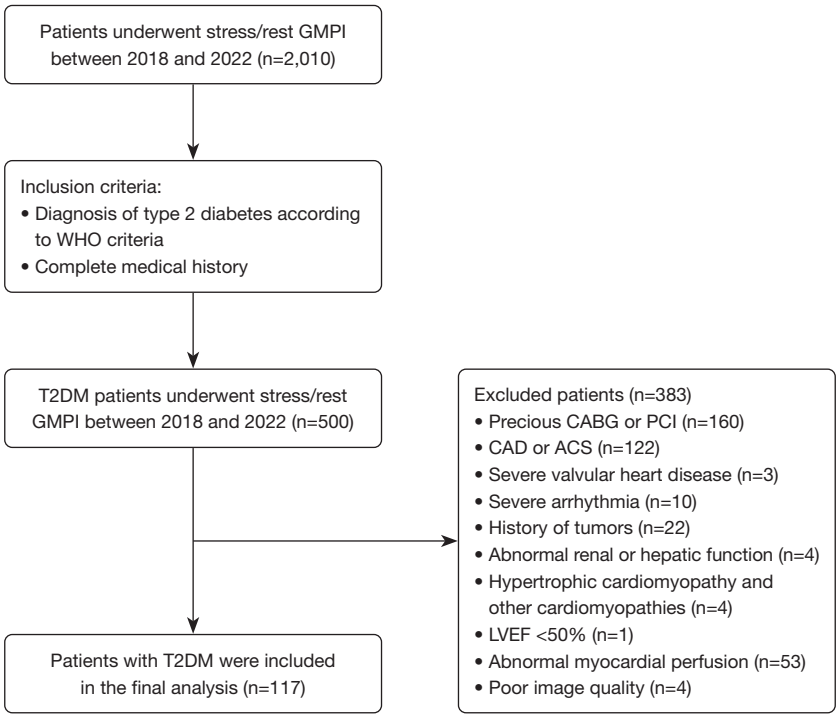

Figure 1 The flowchart. GMPI, gated myocardial perfusion imaging; WHO, World Health Organization; T2DM, type 2 diabetes mellitus; CABG, coronary artery bypass grafting; PCI, percutaneous coronary intervention; CAD, coronary artery disease; ACS, acute coronary syndrome; LVEF, left ventricular ejection fraction.

new imaging marker and potential therapeutic target for early evaluating subclinical myocardial damage. We present this article in accordance with the STROBE reporting checklist (available at https://qims.amegroups.com/article/view/10.21037/qims-23-1413/rc).

Methods

Study population

This was a retrospective study that enrolled T2DM patients who underwent stress-rest gated SPECT-myocardial perfusion imaging (MPI) at The Third Affiliated Hospital of Soochow University from January 2018 to December 2022. The exclusion criteria were as follows: (I) history of coronary revascularization, history of acute coronary syndrome, and coronary artery disease confirmed by coronary angiography. (II) Severe valvular heart disease or severe arrhythmia. (III) History of malignant tumors, (IV) abnormal renal or hepatic function, (V) hypertrophic cardiomyopathy and other cardiomyopathies, (VI) LVEF <50%. (VII) Abnormal MPI by SPECT-CT, (VIII) poor image quality (15). Finally, 117 patients with T2DM with normal LVEF and normal MPI were enrolled for analysis. Additionally, to obtain the reference threshold of LVSD, we also included 83 individuals as a control group who were matched by age and gender and did not have diabetes or cardiovascular disease. *Figure 1* displays the study flowchart. The study was approved by the Ethics Committee of The Third Affiliated Hospital of Soochow University (No. 2023-062) and was conducted according to the Declaration of Helsinki (as revised in 2013). The requirement for informed consent was waived due to the retrospective nature of the study.

Clinical data

Clinical and laboratory data were extracted retrospectively from medical records, including age, gender, height, weight, fasting blood glucose (FBG), glycosylated hemoglobin (HbA1c), triglycerides (TG), total cholesterol (TC), low-density lipoprotein (LDL)-cholesterol, high-density lipoprotein (HDL)-cholesterol, smoking status, alcohol intake, and medications (including statin therapy and

antidiabetic medications). Body mass index (BMI) was calculated as weight in kilograms divided by the square of height in meters. Hypertension was defined as blood pressure (BP) ≥140/90 mmHg or the use of antihypertensive drugs. Hyperlipidemia was defined as TC ≥220 mg/dL, TG ≥150 mg/dL, or history of treatment for hyperlipidemia. Active smoking was defined as the act of currently smoking or having smoked within the past year. Active drinking referred to drinking alcohol at least once a week and lasting for more than 6 months. In addition, we estimated LVEF by echocardiography. All patients underwent echocardiography within 1 month before or after MPI, and the LVEF was evaluated using the modified Simpson method on 2-dimensional echocardiography.

Gated SPECT-MPI acquisition and analysis

Patients underwent a stress/rest protocol using ^{99m}Tc-sestamibi (^{99m}Tc-MIBI). Stress testing included exercise stress MPI based on the Bruce protocol, or pharmacological stress MPI with adenosine intravenously (i.v.) infused at 0.14 mg/kg/min for 6 minutes. After being injected with 740–925 MBq of ^{99m}Tc-MIBI, the patients were scanned with a 2-detector 90° SPECT-CT camera (Symbia T16; Siemens Medical Systems, Erlangen, Germany). Electrocardiogram (ECG)-gated SPECT imaging was performed according to standards of the American Society of Nuclear Cardiology (16). A total of eight frames were obtained in each cardiac cycle by an ECG R-wave trigger. Images were acquired by using a low-energy, high-spatial-resolution parallel hole collimator, with a 128×128 matrix by using a magnification of 1.45, with a 20% window centered around a 140 keV photo peak. The dual detectors rotated 90° each, collectively covering 180°, with an angle step of 6° and 35 seconds at each step. After reconstruction, the horizontal long-axis, vertical long-axis, and short-axis images were obtained. For semiquantitative assessment of myocardial perfusion abnormality, 17-segment visual interpretation of myocardial perfusion images was performed by 2 experienced nuclear physicians using a standard 5-point scoring system (0: normal to 4: absence of tracer uptake). The summed stress score (SSS), summed rest score (SRS), and summed difference score (SDS) were calculated. SSS ≥4 or SDS ≥2 were considered as abnormal (17).

Synchronicity assessment

Automatic phase analysis (ECTb SyncTool version 4.0; Emory University/Syntermed, Atlanta, GA, USA) using raw images of rest gated-MPI was performed for the evaluation of LVSD. Phase standard deviation (PSD; unit: degree) and phase histogram bandwidth (PBW; unit: degree) are two quantitative indices to assess LVSD (18). Based on previous research, LVSD was defined as above the mean + 2 standard deviations (2SDs) of PSD or PBW obtained (19). The mean values of PSD and PBW in the control cohort were 8.74°±2.18° and 8.74°±2.18°, respectively. LVSD is defined as PSD >13.1° or PBW >37.6°.

Measurement of EFV

As the "one-stop shop" examination, SPECT-CT could quantitatively assess EFV through non-contrast CT after performing rest MPI. The CT scan parameters included a tube current of 100 mA, a voltage of 130 kV, and a slice thickness of 3 mm. EFV was quantified with the volume tool (Syngo Volume, Siemens Healthineers, Erlangen, Germany) and was measured using a semi-automatic segmentation technique on every axial slice from the pulmonary artery bifurcation to the diaphragmatic surface of heart. The CT value of –190 to –30 HU is set for adipose tissue (20). The volume of fat (cm^3) selected is automatically calculated.

Statistical analysis

The statistical analyses were carried out through SPSS 25.0 (IBM Corp., Armonk, NY, USA) and R3.4.3 (software packages: glmnet, pROC, rms, and dca; R Foundation for Statistical Computing, Vienna, Austria). Data conforming to a normal distribution were expressed as mean ± SD. Data not conforming to a normal distribution were expressed as median and interquartile range. Normal distribution of data in each group was tested by Shapiro-Wilk test. Continuous variables were compared by using either independent-sample *t*-test or Mann-Whitney *U* test according to normality. Categorical variables were compared using the Pearson's chi-square test. T2DM patients were divided into tertiles according to their EFV levels. Generalized additive model (GAM) and cubic spline smoothing technique were performed to evaluate the association between EFV and LVSD in T2DM patients. Multivariable logistic regression models were produced to assess the association between EFV and LVSD; three models were generated: (I) a univariable model with EFV as a predictor; (II) multivariable-adjusted model 1, adjusted for age and sex; (III) multivariable-adjusted model 2 was constructed

Table 1 Characteristics of T2DM patients with normal MPI and normal LVEF

Characteristics	LVSD group (n=32)	Non-LVSD group (n=85)	P value
Clinical characteristics			
Age (years)	57.38±7.56	56.28±9.19	0.549
Male	23 (71.8)	45 (52.9)	0.064
Body mass index (kg/m^2)	25.83±2.66	23.94±3.13	0.003*
DM duration (years)	8 [1.3, 10.0]	6 [1.5, 11.0]	0.606
Hypertension	11 (34.4)	22 (25.9)	0.344
Active smoking	10 (31.3)	21 (24.7)	0.475
Active drinking	10 (31.3)	14 (16.5)	0.078
FBG (mmol/L)	8.35 [6.42, 12.29]	7.79 [6.25, 11.45]	0.106
HbA1c (%)	8.7 [7.1, 11.3]	8.5 [7, 11.3]	0.326
TG (mmol/L)	2.07 [1.48, 2.87]	1.77 [1.20, 2.40]	0.059
TC (mmol/L)	4.72±1.44	4.78±1.03	0.812
HDL-cholesterol (mmol/L)	0.98 [0.86, 1.11]	0.98 [0.88, 1.25]	0.191
LDL-cholesterol (mmol/L)	2.53±0.83	2.74±0.74	0.219
Hyperlipidemia	21 (65.6)	49 (57.6)	0.433
Medications			
Statin	14 (43.8)	32 (37.6)	0.547
Oral drug	25 (78.1)	62 (72.9)	0.567
Insulin	10 (31.3)	21 (24.7)	0.475
LVEF (%)	64.1±2.5	63.1±3.2	0.136
EFV (cm^3)	142.41±44.17	108.01±38.24	<0.001*

Data are given as mean ± standard deviation (normal distribution), median [Q1 to Q3] (non-normal distribution), or number (%) for categorical variables. *, P<0.05. T2DM, type 2 diabetes mellitus; MPI, myocardial perfusion imaging; LVEF, left ventricular ejection fraction; LVSD, left ventricular systolic dyssynchrony; DM, diabetes mellitus; FBG, fasting blood glucose; HbA1c, glycosylated hemoglobin; TG, triglycerides; TC, total cholesterol; HDL, high-density lipoprotein; LDL, low-density lipoprotein; EFV, epicardial fat volume.

based on our team's interpretation of a broad review of the literature, and adjusted for age, sex, BMI, DM duration, presence of hypertension, active smoking, FBG, HbA1c, and TG (19,21,22). Receiver operating characteristic (ROC) curve analysis was performed to determine the predictive value of EFV for LVSD. All P values were 2-sided, and P values <0.05 were considered statistically significant.

Results

Comparison of baseline characteristics between T2DM patients with LVSD and the non-LVSD group

Baseline characteristics of the T2DM patients (n=117) are shown in *Table 1*. A total of 32 (27.4%) T2DM patients had LVSD. Compared with non-LVSD group, the BMI and EFV were higher in patients with LVSD (25.83±2.66 *vs.* 23.94±3.13 kg/m^2; 142.41±44.17 *vs.* 108.01±38.24 cm^3, respectively, both P<0.05). There were no statistical differences between the LVSD and non-LVSD groups in age, gender, T2DM duration, smoking, alcohol intaking, hypertension, hyperlipidemia history, FBG, HbA1c, lipid profile, LVEF, and the use of statins and hypoglycemic agents (all P>0.05).

Table 2 demonstrates the influence factors of EFV. Age, BMI, hypertension, and proportion of LVSD increased with tertiles of EFV (all P-trend <0.05). The proportions

Table 2 Baseline characteristics stratified by tertiles of EFV

Characteristics	Bottom	Middle	Top	P for trend
EFV, min–max (cm^3)	42.19–96.23	96.52–131.89	132.07–240.53	–
EFV, mean (cm^3)	73.34±16.81	114.71±9.91	164.22±30.31	–
EFV, median (cm^3)	78.60 [58.22, 88.20]	115.80 [105.90, 122.29]	153.53 [140.0, 179.89]	–
Age (years)	55.1±10.2	54.1±6.3	60.6±8.1	0.005*
Male	20 (51.3)	24 (61.5)	24 (61.5)	0.360
Body mass index (kg/m^2)	23±3.3	24.7±2.5	25.7±2.9	<0.001*
DM duration (years)	8 [2, 13]	5 [2, 10]	5 [1, 12]	0.403
Hypertension	6 (15.4)	11 (28.2)	16 (41.0)	0.014*
Active smoking	9 (23.1)	11 (28.2)	10 (25.6)	0.780
Active drinking	6 (15.4)	8 (20.5)	10 (25.6)	0.265
FBG (mmol/L)	9.52 [6.47, 13.17]	7.59 [6.04, 11.31]	8.48 [6.6, 12.3]	0.589
HbA1c (%)	9.7 [7.6, 12.0]	8.1 [6.8, 9.8]	8.2 [7.1, 11.6]	0.261
TG (mmol/L)	1.96 [1.29, 2.73]	1.81 [1.22, 2.57]	1.76 [1.36, 2.15]	0.200
TC (mmol/L)	4.76 [4.21, 5.43]	4.74 [4.08, 5.21]	4.48 [3.80, 5.70]	0.798
HDL-cholesterol (mmol/L)	0.96 [0.88, 1.19]	1.05 [0.90, 1.26]	0.95 [0.83, 1.10]	0.483
LDL-cholesterol (mmol/L)	2.82±0.76	2.69±0.77	2.55±0.78	0.126
Hyperlipidemia	25 (64.1)	19 (48.7)	22 (56.4)	0.494
Statin	17 (43.6)	15 (38.5)	14 (35.9)	0.487
Oral drug	29 (74.4)	26 (66.7)	32 (82.1)	0.438
Insulin	11 (28.2)	9 (23.1)	11 (28.2)	>0.999
LVSD (%)	3 (7.7)	11 (28.2)	18 (46.2)	<0.001*

Data are given as minimum and maximum values (min–max), mean ± standard deviation (normal distribution), median [Q1 to Q3] (non-normal distribution), or number (%) for categorical variables. *, P<0.05. EFV, epicardial fat volume; DM, diabetes mellitus; FBG, fasting blood glucose; HbA1c, glycosylated hemoglobin; TG, triglycerides; TC, total cholesterol; HDL, high-density lipoprotein; LDL, low-density lipoprotein; LVSD, left ventricular systolic dyssynchrony.

of LVSD in the EFV of low, middle, and high were 7.7%, 28.2%, and 46.2%, respectively (P<0.001). A statistical analysis of the comparison between the normal group and the diabetes group is presented in Table S1. *Figure 2* displays the case example.

Univariate and multivariate logistic regression analysis

In univariate logistic regression, BMI and EFV were associated with LVSD [odds ratio (OR) =1.22, 95% confidence interval (CI): 1.06–1.41, P=0.005; OR =1.22, 95% CI: 1.10–1.37, P<0.001, respectively]. In multivariate logistic regression, EFV was the only independent risk factor of LVSD (OR =1.19; 95% CI: 1.06–1.34; P=0.003) (*Table 3*). *Table 4* shows the results of the multivariable logistic regression analysis. In multivariable-adjusted model 1, the probability of LVSD increased by 24% for every 10 cm^3 increase in EFV. In multivariable-adjusted model 2, the probability of LVSD increased by 20% for every 10 cm^3 increase in EFV.

Smooth curve fitting

GAM (*Figure 3*) was performed to visually assess the association between EFV and LVSD after adjusting for age, sex, BMI, DM duration, presence of hypertension, active smoking, FBG, HbA1c, and TG; it turned out that EFV tended to be linearly associated with LVSD.

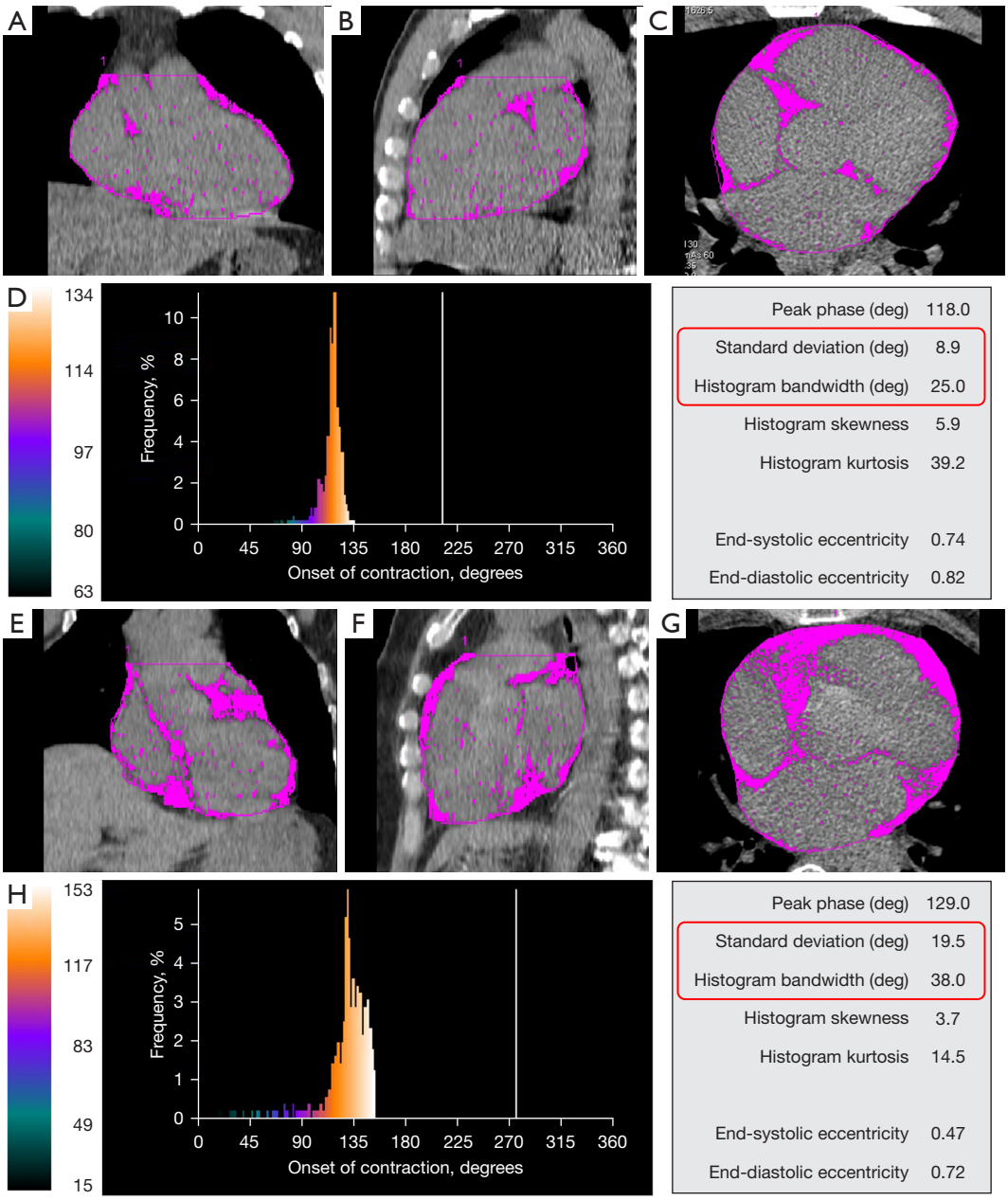

Figure 2 Case examples. (A-D) A 38-year-old T2DM patient in the non-LVSD group with normal myocardial perfusion, normal LVEF (LVEF =63%), and normal EFV. T2DM duration: 6 years; BMI: 26.6 kg/m^2; HbA1c: 7.5%, FBG: 7.59 mmol/L. Panels (A-C) show sagittal, coronal, and transverse sections of a non-contrast CT with EAT in pink and EFV was 79.92 cm^3 (< cutoff value 122.26 cm^3). Panel (D) was the phase histogram, demonstrating synchronous LV contraction with sharp and narrow peak (systolic PSD: 8.9°, systolic PBW: 25°). LVSD was defined as PSD >13.1° or PBW >37.6°. (E-H) A 61-year-old T2DM patient in LVSD group with normal myocardial perfusion, normal LVEF (LVEF =65%) and increased EFV. T2DM duration: 10 years; BMI: 23.4 kg/m^2; HbA1c: 6.7%, FBG: 8.35 mmol/L. Panels (E-G) show sagittal, coronal, and transverse sections of a non-contrast CT with EAT in pink and EFV was 153.41 cm^3, significantly higher than the cut off value of 122.26 cm^3. Panel (H) was the phase histogram, demonstrating LVSD with wide and asymmetry peak (systolic PSD: 19.5°, systolic PBW: 38.0°). PSD and PBW are both higher than the LVSD threshold value. T2DM, type 2 diabetes mellitus; LVSD, left ventricular systolic dyssynchrony; LVEF, left ventricular ejection fraction; BMI, body mass index; HbA1c, glycosylated hemoglobin; FBG, fasting blood glucose; CT, computed tomography; EAT, epicardial adipose tissue; EFV, epicardial fat volume; LV, left ventricular; PSD, phase standard deviation; PBW, phase histogram bandwidth.

Table 3 Univariate and multivariate logistic regression analysis for LVSD

Characteristics	Univariate model			Multivariate model		
	OR	95% CI	P value	OR	95% CI	P value
Age	1.01	0.97–1.06	0.546	–	–	–
Male	2.27	0.94–5.48	0.066	–	–	–
DM duration	1.01	0.95–1.08	0.665	–	–	–
BMI	1.22	1.06–1.41	0.005*	1.14	0.98–1.33	0.085
Hypertension	1.50	0.62–3.60	0.364	–	–	–
Active smoking	1.48	0.60–3.63	0.395	–	–	–
Active drinking	2.31	0.90–5.91	0.082	–	–	–
FBG	1.07	0.97–1.19	0.168	–	–	–
HbA1c	1.06	0.90–1.24	0.491	–	–	–
TG	1.15	0.95–1.34	0.16	–	–	–
Hyperlipidemia	1.41	0.61–3.25	0.416	–	–	–
EFV	1.22	1.10–1.37	<0.001*	1.19	1.06–1.34	0.003*

*, P<0.05. LVSD, left ventricular systolic dyssynchrony; OR, odds ratio; CI, confidence interval; DM, diabetes mellitus; BMI, body mass index; FBG, fasting blood glucose; HbA1c, glycosylated hemoglobin; TG, triglycerides; EFV, epicardial fat volume.

Table 4 Multivariate regression analysis for effect of EFV on LVSD

Groups	Crude model		Multivariable-adjusted model 1		Multivariable-adjusted model 2	
	OR (95% CI)	P value	OR (95% CI)	P value	OR (95% CI)	P value
EFV (per 10 cm^3)	1.22 (1.10, 1.37)	<0.001*	1.24 (1.09, 1.41)	<0.001*	1.20 (1.05, 1.37)	<0.001*
Tertiles						
Bottom tertile (events/N =3/39)	1	–	1	–	1	–
Middle tertile (events/N =11/39)	4.71 (1.20, 18.53)	0.026*	4.51 (1.13, 17.93)	0.032*	4.71 (1.07, 20.67)	0.040*
Top tertile (events/N =18/39)	10.29 (2.71, 39.11)	<0.001*	9.69 (2.42, 38.83)	0.001*	5.60 (1.26, 24.94)	0.024*

Multivariable model 1 was adjusted for age and sex; multivariable model 2 (confounder model) was adjusted for age, sex, BMI, DM duration, presence of hypertension, active smoking, FBG, HbA1c and TG. *, P<0.05. EFV, epicardial fat volume; LVSD, left ventricular systolic dyssynchrony; OR, odds ratio; CI, confidence interval; BMI, body mass index; DM, diabetes mellitus; FBG, fasting blood glucose; HbA1c, glycosylated hemoglobin; TG, triglycerides.

The ROC curve analysis

To assess the predictive value of EFV for LVSD, we performed ROC curve analysis, the area under the curve (AUC) was 0.732 (95% CI: 0.633–0.831, P<0.001) with the optimal cut-off values of EFV (122.26 cm^3) (*Figure 4*). The sensitivity, specificity, positive predictive value (PPV), and negative predictive value (NPV) were 71.9%, 69.4%, 45.8%, and 85.5%, respectively.

Discussion

In this study, we evaluated the relationship between EFV and LVSD in T2DM patients with normal LVEF and normal myocardial perfusion. The main findings were as follows. Firstly, the LVSD group had significantly higher EFV than the non-LVSD group, and multivariate logistic regression analysis showed EFV was the independent risk factor for LVSD. Secondly, a linear relationship

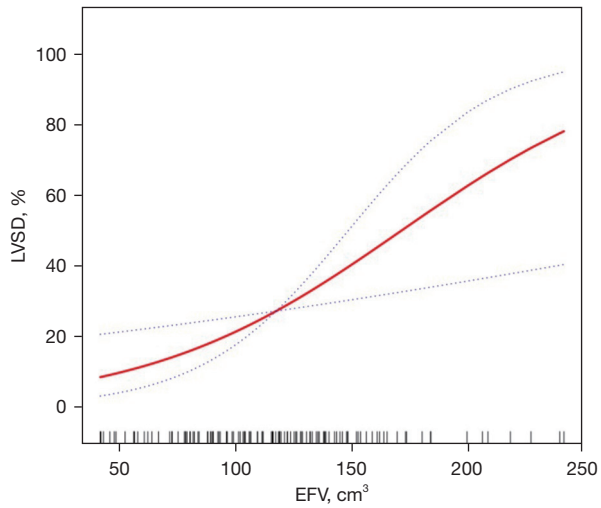

Figure 3 The generalized additive model demonstrated the relationship between EFV and the risk of LVSD after adjusting for age, sex, BMI, diabetes duration, presence of hypertension, active smoking, FBG, HbA1c, and TG. EFV, epicardial fat volume; LVSD, left ventricular systolic dyssynchrony; BMI, body mass index; FBG, fasting blood glucose; HbA1c, glycosylated hemoglobin; TG, triglyceride.

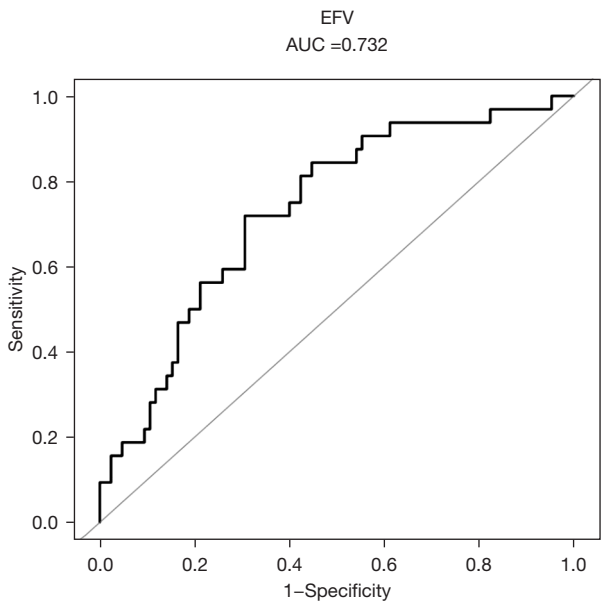

Figure 4 Receiver-operator characteristic curves for prediction of LVSD using EFV. EFV, epicardial fat volume; AUC, area under the curve; LVSD, left ventricular systolic dyssynchrony.

was observed between EFV and LVSD, which remained significant after adjusting for traditional cardiovascular risk factors. For each 10 cm^3 increased in EFV, the risk of LVSD increased by 20.0%. Thirdly, age, BMI, incidence of hypertension, and LVSD were closely associated with EFV and increased with tertiles of EFV. Finally, EFV could effectively predict LVSD at the cutoff value of 122.26 cm^3, with the sensitivity of 71.9% and NPV of 85.5%.

LVSD existed in T2DM patients with normal myocardial perfusion and normal LVEF, which is also known as subclinical myocardial damage and challenging to diagnose early (23,24). Previous studies based on SPECT-MPI have demonstrated that 23–28% of T2DM patients with normal LVEF and normal myocardial perfusion had the presence of LVSD (19,22), which was similar to our findings. A large community-based cohort study found that patients with subclinical myocardial damage have a significantly increased risk of HF and all-cause mortality than those without subclinical myocardial damage (25). Therefore, it is crucial to investigate the factors contributing to early myocardial damage, which may help in diagnostic and treatment decisions, risk stratification, and improve poor prognosis.

Previous studies have found that overweight was independently associated with subclinical myocardial injury quantified by radionuclide MPI and 3-dimensional echocardiography (5,19,26). In addition to measuring systemic fat, we also assessed regional fat distribution by measuring EFV, which is a special visceral adipose tissue located between the myocardium around the heart and the visceral pericardium, and may be a superior marker compared to BMI. We found that LVSD tended to be linearly associated with EFV and the probability of LVSD increased by 20% for every 10 cm^3 increase in EFV after adjusting for confounding factors. Multiple studies have assessed the impact of EAT on subclinical myocardial damage in T2DM patients. Zhu *et al.* observed that EFV measured by MRI was independently linked to left ventricular global peak systolic longitudinal strain and left ventricular peak diastolic longitudinal strain rate (27). However, the measurement of EFV by MRI is limited in clinical application. In another study utilizing ultrasound, Christensen *et al.* found that the thickness of pericardial adipose tissue was associated with impaired global longitudinal strain (28). However, ultrasound has the limitation of reduced objectivity and reproducibility.

The results of our study are similar to those measured by other imaging technologies. SPECT-CT allows for the concurrent assessment of myocardial perfusion and left ventricular systolic synchrony, demonstrating favorable test-retest reliability. In addition to the limitations already discussed, it is important to note that the SPECT-CT utilized in this study does involve exposure to ionizing radiation. However, it does not increase the risk of cancer when the radiation dose is less than 100 mSv. The effective radiation dose for a standard ^{99m}Tc-MIBI imaging (including both rest and stress imaging) is 9–12 mSv, and the dose for a non-contrast CT chest scan (voltage, 130 kV; tube current, 100 mA) to assess CACS and EFV is 1–2 mSv (29).

The pathophysiology connecting EAT to myocardial damage may involve several mechanisms. Firstly, accumulation of EAT may lead to disturbances in glucose and lipid metabolism. EAT has been found to be associated with insulin resistance and metabolic syndrome (30,31). Hyperglycemia damages the myocardium and aggravates mitochondrial dysfunction, and the release of inflammatory factors and oxidative stress (32). The microenvironment of diabetes triggers cellular senescence, leading to excessive release of free fatty acids by adipose tissue, causing lipotoxicity (33). Secondly, as an endocrine organ, EAT secretes various cytokines and pro-inflammatory chemokines, such as tumor necrosis factor-alpha (TNF-α), interleukins (ILs), and adiponectin, directly or indirectly acting on the myocardium and cardiac blood vessels (34). Thirdly, EAT is closely related to coronary microcirculation. The study by Nakanishi *et al.* found the association of periventricular EAT with impaired coronary flow reserve (CFR) and deteriorated left ventricular diastolic function (35). Numerous observational investigations have documented that individuals with T2DM manifest an aberrantly augmented and biologically altered EAT in comparison to their non-diabetic counterparts. This enlarged EAT exerts not only a mechanical constraint on diastolic filling but also serves as a reservoir for pro-inflammatory mediators, which have the potential to induce inflammation, microcirculatory dysfunction, and fibrosis within the subjacent myocardium. Consequently, these pathological processes impede the relaxability of the left ventricle and escalate its filling pressure (36).

Using a threshold value of 122.26 cm^3, EFV could effectively predict LVSD with the AUC, sensitivity, and specificity of 0.73, 71.9%, and 69.4% respectively. Similarly, Maimaituxun *et al.* found that in patients with normal LVEF, EFV showed a significant power for predicting myocardial dysfunction using GLS ≤18 by ultrasound as the reference with the cutoff value of 116 cm^3 and the AUC, sensitivity, and specificity were 0.60, 62.3%, and 60.6%, respectively (37). Therefore, T2DM patients with excess EFV may need appropriate intervention to prevent subclinical myocardial damage and further deterioration of left ventricular function. Since EAT is a modifiable factor, therapeutic strategies are targeted to reduce EAT. For example, both glucagon-like-peptide-1 receptor agonists (GLP-1) and inhibitors of sodium glucose cotransporter 2 (SGLT2i) exhibit the potential to decrease the accumulation of EAT and provide further cardiovascular benefits (38,39). EAT may be a potential therapeutic target for subclinical myocardial damage and whether the LVSD could be improved after reducing EFV accumulation needs further verification. Besides, it has been confirmed that SGLT2i can significantly improve the longitudinal strain of T2DM in the early stage (40), whether the efficacy can be ascribed to the direct effect on EAT still requires further study.

Our study has several limitations. Firstly, it is a single-center retrospective observational study with a small sample size. Future detailed prospective studies with larger samples are necessary to further investigate the potential causal relationship between EFV and subclinical myocardial damage in people with diabetes. Secondly, due to limitations in laboratory conditions, various adipokines and pro-inflammatory factors related to EAT were not detected. Thirdly, we did not conduct oral glucose tolerance tests or glucose clamp studies to measure insulin resistance. As insulin resistance plays a central pathophysiological role in the possible correlation between epicardial fat and subclinical myocardial damage in patients with T2DM, the relationship between the accumulation of epicardial fat, insulin resistance, and subclinical myocardial damage deserves further research. Fourthly, there is a lack of measurements of waist or hip circumference. Finally, due to a lack of follow-up assessments, the prognostic value of EFV remains unknown.

Conclusions

EFV is an independent risk factor for LVSD in T2DM patients with normal LVEF and normal MPI, which could serve as a novel imaging marker and a potential therapeutic target for subclinical myocardial damage.

New knowledge gained

In the present study, we elucidated the relationship between

EFV and LVSD in T2DM patients with normal LVEF and normal myocardial perfusion. We concluded that EFV was the independent risk factor for LVSD in T2DM patients with normal LVEF and normal MPI, which might serve as a novel imaging marker and a potential therapeutic target for subclinical myocardial damage.

Acknowledgments

Funding: This research was supported by the National Natural Science Foundation of China (Nos. 82272031 and 81871381, PI: Yuetao Wang), Key Research and Development Program of Jiangsu Province (Social Development) (Grant No. BE2021638), Top Talent of Changzhou "The 14th Five-Year Plan"High-Level Health Talents Training Project [No. (2022)260], Changzhou Clinical Medical Center [(2022)261], the Science and Technology Project for Youth Talents of Changzhou Health Committee (No. QN202212, PI: Wenji Yu), and Young Talent Development Plan of Changzhou Health Commission (No. CZQM2023008, PI: Wenji Yu).

Footnote

Reporting Checklist: The authors have completed the STROBE reporting checklist. Available at https://qims.amegroups.com/article/view/10.21037/qims-23-1413/rc

Conflicts of Interest: All authors have completed the ICMJE uniform disclosure form (available at https://qims.amegroups.com/article/view/10.21037/qims-23-1413/coif). The authors have no conflicts of interest to declare.

Ethical Statement: The authors are accountable for all aspects of the work in ensuring that questions related to the accuracy or integrity of any part of the work are appropriately investigated and resolved. The study was conducted in accordance with the Declaration of Helsinki (as revised in 2013) and approved by the Ethics Committee of The Third Affiliated Hospital of Soochow University (No. 2023-062). The requirement for informed consent was waived due to the retrospective nature of the study.

References

1. Sun H, Saeedi P, Karuranga S, Pinkepank M, Ogurtsova K, Duncan BB, Stein C, Basit A, Chan JCN, Mbanya JC, Pavkov ME, Ramachandaran A, Wild SH, James S, Herman WH, Zhang P, Bommer C, Kuo S, Boyko EJ, Magliano DJ. IDF Diabetes Atlas: Global, regional and country-level diabetes prevalence estimates for 2021 and projections for 2045. Diabetes Res Clin Pract 2022;183:109119.
2. Ritchie RH, Abel ED. Basic Mechanisms of Diabetic Heart Disease. Circ Res 2020;126:1501-25.
3. Murtaza G, Virk HUH, Khalid M, Lavie CJ, Ventura H, Mukherjee D, Ramu V, Bhogal S, Kumar G, Shanmugasundaram M, Paul TK. Diabetic cardiomyopathy - A comprehensive updated review. Prog Cardiovasc Dis 2019;62:315-26.
4. Lorenzo-Almorós A, Tuñón J, Orejas M, Cortés M, Egido J, Lorenzo Ó. Diagnostic approaches for diabetic cardiomyopathy. Cardiovasc Diabetol 2017;16:28.
5. Wang Y, Yu W, Yang X, Zhang F, Sun Y, Hu Y, Yang L, Jiang Q, Wang J, Shao X, Wang Y. Left ventricular systolic dyssynchrony: a novel imaging marker for early assessment of myocardial damage in Chinese type 2 diabetes mellitus patients with normal left ventricular ejection fraction and normal myocardial perfusion. J Nucl Cardiol 2023;30:1797-809.
6. Nagueh SF. Mechanical dyssynchrony in congestive heart failure: diagnostic and therapeutic implications. J Am Coll Cardiol 2008;51:18-22.
7. Fudim M, Dalgaard F, Fathallah M, Iskandrian AE, Borges-Neto S. Mechanical dyssynchrony: How do we measure it, what it means, and what we can do about it. J Nucl Cardiol 2021;28:2174-84.
8. Hage FG. Left ventricular mechanical dyssynchrony by phase analysis as a prognostic indicator in heart failure. J Nucl Cardiol 2014;21:67-70.
9. Iacobellis G. Epicardial adipose tissue in contemporary cardiology. Nat Rev Cardiol 2022;19:593-606.
10. Yu W, Liu B, Zhang F, Wang J, Shao X, Yang X, Shi Y, Wang B, Xu Y, Wang Y. Association of Epicardial Fat Volume With Increased Risk of Obstructive Coronary Artery Disease in Chinese Patients With

Suspected Coronary Artery Disease. J Am Heart Assoc 2021;10:e018080.
11. Arshi B, Aliahmad HA, Ikram MA, Bos D, Kavousi M. Epicardial Fat Volume, Cardiac Function, and Incident Heart Failure: The Rotterdam Study. J Am Heart Assoc 2023;12:e026197.
12. van Rosendael AR, Smit JM, El'Mahdiui M, van Rosendael PJ, Leung M, Delgado V, Bax JJ. Association between left atrial epicardial fat, left atrial volume, and the severity of atrial fibrillation. Europace 2022;24:1223-8.
13. Liu J, Li J, Pu H, He W, Zhou X, Tong N, Peng L. Cardiac remodeling and subclinical left ventricular dysfunction in adults with uncomplicated obesity: a cardiovascular magnetic resonance study. Quant Imaging Med Surg 2022;12:2035-50.
14. Muzurović EM, Vujošević S, Mikhailidis DP. Can We Decrease Epicardial and Pericardial Fat in Patients With Diabetes? J Cardiovasc Pharmacol Ther 2021;26:415-36.
15. Jellis CL, Sacre JW, Wright J, Jenkins C, Haluska B, Jeffriess L, Martin J, Marwick TH. Biomarker and imaging responses to spironolactone in subclinical diabetic cardiomyopathy. Eur Heart J Cardiovasc Imaging 2014;15:776-86.
16. Henzlova MJ, Duvall WL, Einstein AJ, Travin MI, Verberne HJ. ASNC imaging guidelines for SPECT nuclear cardiology procedures: Stress, protocols, and tracers. J Nucl Cardiol 2016;23:606-39.
17. Driessen RS, Raijmakers PG, Danad I, Stuijfzand WJ, Schumacher SP, Leipsic JA, Min JK, Knuuti J, Lammertsma AA, van Rossum AC, van Royen N, Underwood SR, Knaapen P. Automated SPECT analysis compared with expert visual scoring for the detection of FFR-defined coronary artery disease. Eur J Nucl Med Mol Imaging 2018;45:1091-100.
18. Chen J, Garcia EV, Bax JJ, Iskandrian AE, Borges-Neto S, Soman P. SPECT myocardial perfusion imaging for the assessment of left ventricular mechanical dyssynchrony. J Nucl Cardiol 2011;18:685-94.
19. Malik D, Mittal B, Sood A, Parmar M, Kaur G, Bahl A. Left ventricular mechanical dyssynchrony assessment in long-standing type II diabetes mellitus patients with normal gated SPECT-MPI. J Nucl Cardiol 2019;26:1650-8.
20. Huang G, Wang D, Zeb I, Budoff MJ, Harman SM, Miller V, Brinton EA, El Khoudary SR, Manson JE, Sowers MR, Hodis HN, Merriam GR, Cedars MI, Taylor HS, Naftolin F, Lobo RA, Santoro N, Wildman RP. Intra-thoracic fat, cardiometabolic risk factors, and subclinical cardiovascular disease in healthy, recently menopausal women screened for the Kronos Early Estrogen Prevention Study (KEEPS). Atherosclerosis 2012;221:198-205.
21. Song XT, Wang SK, Zhang PY, Fan L, Rui YF. Association between epicardial adipose tissue and left ventricular function in type 2 diabetes mellitus: Assessment using two-dimensional speckle tracking echocardiography. J Diabetes Complications 2022;36:108167.
22. Hosseinzadeh E, Ghodsirad MA, Alirezaei T, Arfenia M, Pirayesh, Amoiee M, Norouzi GH. Comparing left ventricular mechanical dyssynchrony between diabetic and non-diabetic patients with normal gated SPECT MPI. Int J Cardiovasc Imaging 2022;38:249-56.
23. Nappi C, Gaudieri V, Acampa W, Assante R, Zampella E, Mainolfi CG, Petretta M, Germano G, Cuocolo A. Comparison of left ventricular shape by gated SPECT imaging in diabetic and nondiabetic patients with normal myocardial perfusion: A propensity score analysis. J Nucl Cardiol 2018;25:394-403.
24. Gaudieri V, Nappi C, Acampa W, Zampella E, Assante R, Mannarino T, Genova A, De Simini G, Klain M, Germano G, Petretta M, Cuocolo A. Added prognostic value of left ventricular shape by gated SPECT imaging in patients with suspected coronary artery disease and normal myocardial perfusion. J Nucl Cardiol 2019;26:1148-56.
25. Selvin E, Lazo M, Chen Y, Shen L, Rubin J, McEvoy JW, Hoogeveen RC, Sharrett AR, Ballantyne CM, Coresh J. Diabetes mellitus, prediabetes, and incidence of subclinical myocardial damage. Circulation 2014;130:1374-82.
26. Wu T, Gong L, Zhang C, Zhang D, Li X. Three-dimensional echocardiography and strain cardiac imaging in patients with prediabetes and type 2 diabetes mellitus. Quant Imaging Med Surg 2023;13:7753-64.
27. Zhu J, Li W, Xie Z, Zhuo K. Relationship Between Epicardial Adipose Tissue and Biventricular Longitudinal Strain and Strain Rate in Patients with Type 2 Diabetes Mellitus. Acad Radiol 2023;30:833-40.
28. Christensen RH, Hansen CS, von Scholten BJ, Jensen MT, Pedersen BK, Schnohr P, Vilsbøll T, Rossing P, Jørgensen PG. Epicardial and pericardial adipose tissues are associated with reduced diastolic and systolic function in type 2 diabetes. Diabetes Obes Metab 2019;21:2006-11.
29. Salvatori M, Rizzo A, Rovera G, Indovina L, Schillaci O. Radiation dose in nuclear medicine: the hybrid imaging. Radiol Med 2019;124:768-76.
30. Cerit Z. Like two peas in a pod: Metabolic syndrome and epicardial obesity. Diabetes Metab Syndr 2018;12:477.
31. Levelt E, Pavlides M, Banerjee R, Mahmod M, Kelly

C, Sellwood J, Ariga R, Thomas S, Francis J, Rodgers C, Clarke W, Sabharwal N, Antoniades C, Schneider J, Robson M, Clarke K, Karamitsos T, Rider O, Neubauer S. Ectopic and Visceral Fat Deposition in Lean and Obese Patients With Type 2 Diabetes. J Am Coll Cardiol 2016;68:53-63.
32. Gandoy-Fieiras N, Gonzalez-Juanatey JR, Eiras S. Myocardium Metabolism in Physiological and Pathophysiological States: Implications of Epicardial Adipose Tissue and Potential Therapeutic Targets. Int J Mol Sci 2020;21:2641.
33. Molinaro C, Salerno L, Marino F, Scalise M, Salerno N, Pagano L, De Angelis A, Cianflone E, Torella D, Urbanek K. Unraveling and Targeting Myocardial Regeneration Deficit in Diabetes. Antioxidants (Basel) 2022;11:208.
34. Gaborit B, Sengenes C, Ancel P, Jacquier A, Dutour A. Role of Epicardial Adipose Tissue in Health and Disease: A Matter of Fat? Compr Physiol 2017;7:1051-82.
35. Nakanishi K, Fukuda S, Tanaka A, Otsuka K, Taguchi H, Shimada K. Relationships Between Periventricular Epicardial Adipose Tissue Accumulation, Coronary Microcirculation, and Left Ventricular Diastolic Dysfunction. Can J Cardiol 2017;33:1489-97.
36. Salvatore T, Galiero R, Caturano A, Vetrano E, Rinaldi L, Coviello F, Di Martino A, Albanese G, Colantuoni S, Medicamento G, Marfella R, Sardu C, Sasso FC. Dysregulated Epicardial Adipose Tissue as a Risk Factor and Potential Therapeutic Target of Heart Failure with Preserved Ejection Fraction in Diabetes. Biomolecules 2022;12:176.
37. Maimaituxun G, Kusunose K, Yamada H, Fukuda D, Yagi S, Torii Y, Yamada N, Soeki T, Masuzaki H, Sata M, Shimabukuro M. Deleterious Effects of Epicardial Adipose Tissue Volume on Global Longitudinal Strain in Patients With Preserved Left Ventricular Ejection Fraction. Front Cardiovasc Med 2020;7:607825.
38. Iacobellis G, Baroni MG. Cardiovascular risk reduction throughout GLP-1 receptor agonist and SGLT2 inhibitor modulation of epicardial fat. J Endocrinol Invest 2022;45:489-95.
39. Dozio E, Vianello E, Malavazos AE, Tacchini L, Schmitz G, Iacobellis G, Corsi Romanelli MM. Epicardial adipose tissue GLP-1 receptor is associated with genes involved in fatty acid oxidation and white-to-brown fat differentiation: A target to modulate cardiovascular risk? Int J Cardiol 2019;292:218-24.
40. Oka S, Kai T, Hoshino K, Watanabe K, Nakamura J, Abe M, Watanabe A. Effects of empagliflozin in different phases of diabetes mellitus-related cardiomyopathy: a prospective observational study. BMC Cardiovasc Disord 2021;21:217.

Cite this article as: Hu Y, Yu W, Zhang F, Wang Y, Wang J, Wan P, Shao X, Wang J, Sun Y, Wang Y. Association of epicardial fat volume with subclinical myocardial damage in patients with type 2 diabetes mellitus. Quant Imaging Med Surg 2024;14(3):2627-2639. doi: 10.21037/qims-23-1413

Supplementary

Table S1 Comparison of baseline characteristics between normal group and T2DM group

Characteristics	Normal group (n=83)	T2DM group (n=117)	P value
Age (years)	57.71±10.14	56.58±8.75	0.401
Male	42 (50.6)	68 (58.1)	0.292
BMI (kg/m^2)	23.77±3.47	24.46±3.11	0.142
Active smoking	18 (21.7)	30 (25.6)	0.519
Active drinking	5 (6.0)	24 (20.5)	0.004*
FBG (mmol/L)	5.11 [4.72, 5.53]	8.35 [6.42, 12.29]	<0.001*
TG (mmol/L)	1.57 [1.16, 1.93]	1.82 [1.29, 2.55]	0.025*
TC (mmol/L)	4.33±0.77	4.76±1.15	0.002*
HDL-cholesterol (mmol/L)	1.10 [0.95, 1.28]	0.98 [0.87, 1.18]	0.031*
LDL-cholesterol (mmol/L)	2.43±0.60	2.69±0.77	0.009*
PSD (°)	8.5 [7.4, 10.3]	10 [8.2, 12.15]	<0.001*
PBW (°)	27 [24, 30]	30 [25, 36.5]	<0.001*

Data are given as mean ± standard deviation (normal distribution), median [Q1 to Q3] (non-normal distribution), or number (%) for categorical variables. *, P<0.05. T2DM, type 2 diabetes mellitus; BMI, body mass index; FBG, fasting blood glucose; TG, triglycerides; TC, total cholesterol; HDL, high-density lipoprotein; LDL, low-density lipoprotein; PSD, phase standard deviation; PBW, phase histogram bandwidth.

https://dx.doi.org/10.21037/qims-23-1413